JACS
JOURNAL OF THE AMERICAN CHEMICAL SOCIETY

Article

pubs.acs.org/JACS

Characterization of a C3 Deoxygenation Pathway Reveals a Key Branch Point in Aminoglycoside Biosynthesis

Meinan Lv,[†,#] Xinjian Ji,[‡,#] Junfeng Zhao,[†,‡] Yongzhen Li,[‡] Chen Zhang,[‡] Li Su,[†] Wei Ding,[‡] Zixin Deng,[†] Yi Yu,[*,†] and Qi Zhang[*,‡]

[†]Key Laboratory of Combinatory Biosynthesis and Drug Discovery (Ministry of Education), School of Pharmaceutical Sciences, Wuhan University, Wuhan, 430071, China

[‡]Department of Chemistry, Fudan University, Shanghai, 200433, China

Supporting Information

ABSTRACT: Apramycin is a clinically interesting aminoglycoside antibiotic (AGA) containing a highly unique bicyclic octose moiety, and this octose is deoxygenated at the C3 position. Although the biosynthetic pathways for most 2-deoxystreptamine-containing AGAs have been well characterized, the pathway for apramycin biosynthesis, including the C3 deoxygenation process, has long remained unknown. Here we report detailed investigation of apramycin biosynthesis by a series of genetic, biochemical and bioinformatical studies. We show that AprD4 is a novel radical *S*-adenosyl-L-methionine (SAM) enzyme, which uses a noncanonical CX_3CX_3C motif for binding of a [4Fe-4S] cluster and catalyzes the dehydration of paromamine, a pseudodisaccharide intermediate in apramycin biosynthesis. We also show that AprD3 is an NADPH-dependent reductase that catalyzes the reduction of the dehydrated product from AprD4-catalyzed reaction to generate lividamine, a C3′ deoxygenated product of paromamine. AprD4 and AprD3 do not form a tight catalytic complex, as shown by protein complex immunoprecipitation and other assays. The AprD4/AprD3 enzyme system acts on different pseudodisaccharide substrates but does not catalyze the deoxygenation of oxyapramycin, an apramycin analogue containing a C3 hydroxyl group on the octose moiety, suggesting that oxyapramycin and apramycin are partitioned into two parallel pathways at an early biosynthetic stage. Functional dissection of the C6 dehydrogenase AprQ shows the crosstalk between different AGA biosynthetic gene clusters from the apramycin producer *Streptomyces tenebrarius*, and reveals the remarkable catalytic versatility of AprQ. Our study highlights the intriguing chemistry in apramycin biosynthesis and nature's ingenuity in combinatorial biosynthesis of natural products.

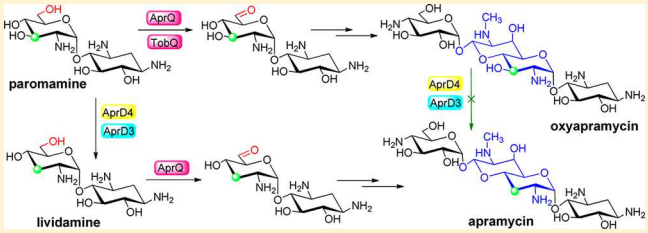

INTRODUCTION

Aminoglycoside antibiotics (AGAs) constitute a large class of clinically important antibiotics.[1−3] By specifically interacting with bacterial rRNAs and inhibiting protein synthesis,[4,5] this class of compounds exhibit potent activity against a broad spectrum of Gram positive and negative pathogens, and have been widely used to treat bacterial infections for many years. Although the importance of AGAs has waned in the last 2 decades due to the emergence of other antibiotics with fewer side effects, there is a renewed clinical interest in AGAs, as they represent one of the few remaining treatment options, particularly for Gram negative bacteria.[2,3] A clinically promising AGA member is apramycin,[6] which mimics the features of an incompatible plasmid and thereby resensitizes bacteria to conventional antibiotic treatments by causing plasmid elimination in vivo.[7] This novel mode of action of apramycin suggests a potentially useful strategy for combating drug-resistant pathogenic bacteria. Moreover, in contrast to common AGAs that possess substantial ototoxicity and could cause irreversible hearing loss,[3] recent studies have shown that apramycin has only little ototoxicity in the ex vivo cultures of cochlear explants and in the in vivo guinea pig model,[8] demonstrating the potential in developing apramycin for clinical applications.[2,9]

Apramycin (**1**) contains a 4-monosubstituted 2-deoxystreptamine (2-DOS) and a highly unique bicyclic octose moiety, and the latter is deoxygenated at the C3 position (Figure 1). Biosynthesis of the 2-DOS-containing AGAs has been extensively studied during the past decade, and most of their biosynthetic pathways have been well established.[10−12] In contrast, the pathway for apramycin biosynthesis remains largely elusive. In the seminal pioneering work by Piepersberg et al.,[1,13] it was hypothesized that an NDP-activated octose is synthesized and subsequently attached to the 4-amino group of 2-DOS, whereas in anther hypothesis, the octose is assembled from a pseudodisaccharide intermediate paromamine (**2**) (Figure 1).[10,14] Both hypotheses imply that the C3′ deoxygenation of the octose moiety occurs at a very late stage of apramycin biosynthesis (Figure 1). In this work, we report detailed investigation of apramycin biosynthesis by a series of genetic and biochemical studies complemented by

Received: December 26, 2015
Published: April 27, 2016

DOI: 10.1021/jacs.6b02221
J. Am. Chem. Soc. 2016, 138, 6427−6435

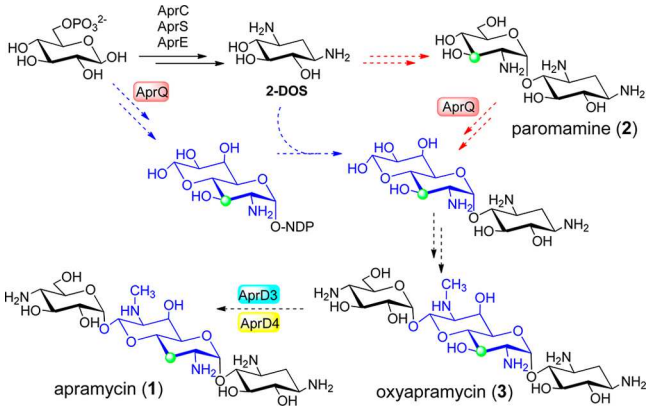

Figure 1. Previously proposed pathways of apramycin biosynthesis. Biosynthesis of 2-DOS has been well characterized in other 2-DOS-containing AGAs (e.g., butirosin, kanamycin) and is shown by solid arrows. The uncharacterized steps are shown by dashed arrows, among which the two different hypothesized pathways are shown in red and blue, respectively. The octose moieties are shown in blue, and the C3 positions are shown by green spheres. The enzymes investigated in detail in this work are highlighted by colored boxes.

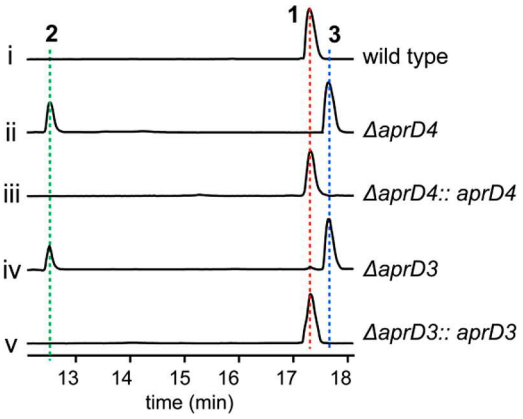

Figure 2. Identification of paromamine as the substrate for C3 deoxygenation, showing the HPLC traces of the culture extracts from (i) *S. tenebrarius* wild type strain, (ii) the Δ*aprD4* mutant, (iii) the Δ*aprD4* mutant containing an *aprD4*-expressing plasmid, (iv) the Δ*aprD3* mutant, and (v) the Δ*aprD3* mutant containing an *aprD3*-expressing plasmid. The HPLC analysis was performed by using an evaporative light-scattering detector (ELSD).

bioinformatical analysis. These investigations allowed us to characterize an unprecedented sugar C3 deoxygenation pathway in detail and reveal a key branch point in AGA biosynthesis.

RESULTS

Identification of Paromamine As the Substrate for C3 Deoxygenation. C3 deoxygenation in apramycin biosynthesis is presumably catalyzed by a putative dehydrogenase AprD3 and a putative Fe−S oxidoreductase AprD4.[10,15,16] Coexpression of *aprD3* and *aprD4* with kanamycin biosynthetic genes resulted in production of novel 3′-deoxykanamycins, and conversion of neamine to nebramine was observed by using the cell free extract of *S. venezuelae* expressing *aprD4* and *aprD3*.[16] These results support the involvement of AprD3 and AprD4 in C3 deoxygenation (Figure 1). To interrogate the function of AprD4, we knocked out its encoding gene from the apramycin producer *Streptomyces tenebrarius* by targeted in-frame deletion of the 1059-bp internal fragment (Figure S1). High resolution (HR)-liquid chromatography (LC)-mass spectrometry (MS) analysis showed that apramycin production was completely abolished in the Δ*aprD4* mutant, and this was concomitant with significantly enhanced production (~20 mg/L) of a compound with a retention time similar to that of apramycin (Figure 2, trace (ii)) and a protonated molecular ion at m/z = 556.2821 (1.6 ppm error for a calculated molecule formula of $C_{21}H_{41}N_5O_{12}$). Large scale of fermentation, purification, and detailed structural characterization using HR-MS/MS, ^{1}HNMR and ^{13}CNMR analysis confirmed that this product is oxyapramycin (**3**) (Figure S2−S4), an apramycin analogue whose C3′ is not deoxygenated (Figure 1). Oxyapramycin is also produced by the *S. tenebrarius* wild type strain in a low yield, and was believed to be an intermediate in apramycin biosynthesis (Figure 1). We also observed the production of another compound (~5 mg/L) in the culture of the Δ*aprD4* mutant, and this compounds was eluted at a time quite earlier than that of apramycin (Figure 2, trace (ii)) and exhibited a protonated molecular ion at m/z = 324.1769. Its suggested molecule formula $C_{12}H_{25}N_3O_7$ ($[M + H]^+$ calc. 324.1771, 0.6 ppm error) is consistent with paromamine (**2**) (Figure 1), and this proposal was validated by HR-MS/MS, ^{1}H NMR, and ^{13}C NMR analysis of the purified compound (Figure S5−S7). Introduction of an *aprD4*-expressing plasmid into the mutant dramatically diminished the production of oxyapramycin and paromamine, and restored apramycin production to the wide type level (~23 mg/L) (Figure 2, trace (iii)). These results demonstrated the strict requirement of AprD4 for C3 deoxygenation and suggested that paromamine is an intermediate in apramycin biosynthesis. The apparent production of paromamine by the Δ*aprD4* mutant suggested that paromamine (**2**), not oxyapramycin (**3**), is the likely substrate for C3 deoxygenation.

AprD4 Is a Novel Radical SAM Dehydratase. AprD4 has a highest similarity (BlastP E-value = 1.1×10^{-31}) with proteins belong to the TIGR03471 family. This protein family consists of the homologues of the radical SAM protein HpnJ, which was proposed to catalyze the conversion of a glucosamine moiety to a 5-membered cyclitol in hopanoid biosynthesis.[17] Radical SAM enzymes are a large and rapidly growing superfamily that utilizes a [4Fe-4S] cluster to bind SAM and reductively cleave its carbon−sulfur bond. The 5′-deoxyadenosyl (dAdo) radical produced by this way is highly reactive, which typically abstracts a hydrogen atom from its reaction partner and initiates a remarkably diverse variety of reactions.[18−28]

To study AprD4 in vitro, we overexpressed the enzyme in *E. coli* with an N-terminal hexa-His tag and purified it by Ni^{2+}-affinity chromatography. The aerobically purified protein had a pale brownish color, suggesting it is likely a Fe−S protein. We therefore purified the protein and chemically reconstituted the Fe−S cluster under a strictly anaerobic condition. When the reconstituted AprD4 was incubated with SAM and sodium dithionite, production of 5′-deoxyadenosine (dAdoH), the trademark product of radical SAM enzymes, was observed (Figure 3A, trace (ii)), and its production was dramatically enhanced when paromamine was added to the reaction (Figure 3A, trace (iii)), indicating that AprD4 is a member of the radical SAM enzyme superfamily.

AprD4 has 12 Cys residues but does not have an N-terminal CX_3CX_2C motif found in most of the radical SAM superfamily enzymes.[18−21] Instead, AprD4 contains a CPYPCRFYC (CX_3CX_3C) motif in the middle of the enzyme sequence,

DOI: 10.1021/jacs.6b02221
J. Am. Chem. Soc. 2016, 138, 6427−6435

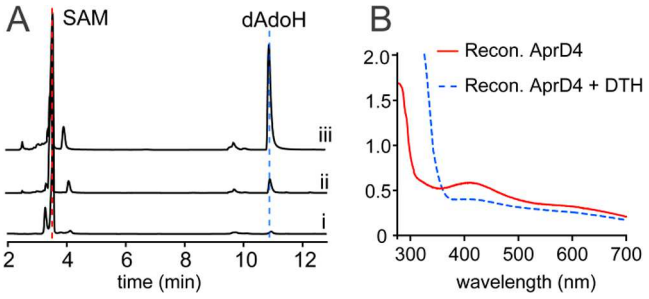

Figure 3. Characterization of AprD4 as a radical SAM enzyme. (A) HPLC analysis of the SAM cleavage activity of AprD4 (i) without addition of dithionite (DTH), (ii) with DTH, and (iii) with DTH and paromamine. For trace iii, assay was carried out by incubating 1 mM SAM with ca. 50 μM reconstituted protein, 500 μM paromamine, and 2 mM sodium dithionite in 50 mM MOPS buffer (pH 8.0) for 5 h, and dAdoH produced in the reaction is ca. 400 μM. (B) UV−vis spectra of the reconstituted AprD4 (red solid line) and the protein reduced with DTH (blue dashed line).

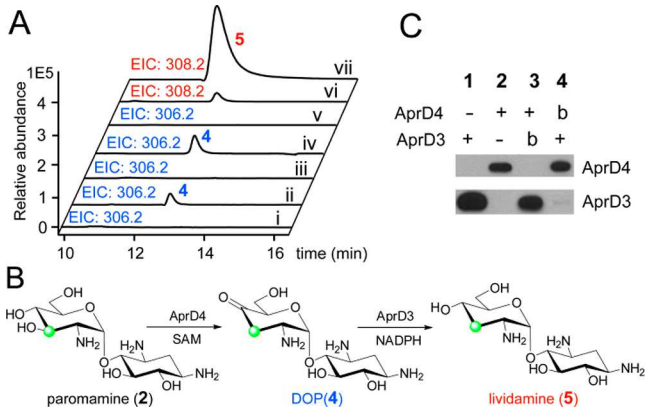

Figure 4. Characterization of AprD4/AprD3 as a novel C3 deoxygenation machinery. (A) LC−MS analysis of AprD4 and AprD3 in vitro activity, showing the extracted ion chromatograms (EICs) of $[M + H]^+$ = 306.2 (corresponding to DOP, **4**) for (i) control reaction in which SAM was omitted, (ii) AprD4 reaction, (iii) AprD4 reaction treated with 0.1 M $NaBH_4$ for ∼1 h, (iv) the culture extracts from the Δ*aprD3* mutant strain, and (v) tandem reaction with AprD4 and AprD3; and the EICs of $[M + H]^+$ = 308.2 (corresponding to the reduced DOP or lividamine) for (vi) AprD4 reaction treated with 0.1 M $NaBH_4$ for ∼1 h (the same reaction as trace (iii)), and (vii) tandem reaction with AprD4 and AprD3 (the same reaction as trace (v)). (B) Paromamine C3′ deoxygenation catalyzed by the sequential action of the radical SAM dehydratase AprD4 and the NADPH-dependent reductase AprD3. (C) Western blot analysis showing that AprD4 and AprD3 do not form tight protein−protein complex. Lane 1 is the cell lysate overexpressing N-terminally Flag-tagged AprD3, whereas lane 2 is the reconstituted AprD4 (His-tagged); lane 3 and 4 are the pull down assays using AprD3 as a bait (b) (i.e., using anti-Flag antibody) and AprD4 as a bait (b) (i.e., using anti-His antibody), respectively. Anti-Flag and anti-His antibodies were used for staining of AprD3 and AprD4, respectively.

which is likely the site for [4Fe-4S] cluster binding. To reveal the [4Fe-4S] binding motif in AprD4, we carried out an Ala scan mutagenesis and replaced each of the 12 Cys residues in AprD4 by Ala. All these mutant proteins were anaerobically purified, chemically reconstituted, and used in the assays same to that for the wild type enzyme. HPLC analysis of the resulting assay mixture showed that the SAM cleavage activity retained for all the 9 mutants in which the CPYPCRFYC motif remained unaltered (Figure S8). However, replacing any of the 3 Cys residues in the CPYPCRFYC motif with Ala (i.e., C203A, C207A, and C211A) rendered the enzyme incapable for SAM cleavage (Figure S8), supporting that the [4Fe-4S] cluster of AprD4 binds to a noncanonical CX_3CX_3C motif.

UV−vis spectroscopy analysis showed that the protein solution had a broad absorption shoulder centered around 410 nm, and this absorption disappeared after addition of sodium dithionite (DTH) into the solution (Figure 3B). Iron and sulfur quantification showed that the reconstituted protein contains 8.1 ± 0.4 mol Fe and 7.9 ± 0.5 mol S per mol protein. We next performed UV−vis spectroscopy analysis with the C207A mutant, in which the CX_3CX_3C motif is impaired. The result showed that the mutant protein also exhibited a broad absorption shoulder centered around 410 nm, which disappeared upon dithionite reduction (Figure S9). Quantitative analysis showed that the C207A mutant contains 6.1 ± 0.4 mol Fe and 5.3 ± 0.4 mol S per mol protein. These results suggested that AprD4 likely contains two [4Fe-4S] clusters.

The reaction mixture containing SAM, paromamine, sodium dithionite, and the reconstituted AprD4 was then subjected to HR-LC−MS analysis, which revealed a new product with a protonated molecular ion at m/z = 306.1663 (Figure 4A, trace (ii)). The suggested molecule formula of the product is $C_{12}H_{23}N_3O_6$ ($[M + H]^+$ calc. 306.1665, 0.6 ppm error), consistent with 3′-deoxy-4′-oxoparomamine (DOP, **4**), a dehydrated product of paromamine (Figure. 4B). HR-MS/MS analysis supported this analysis, showing that dehydration did not occur on the 2-deoxystreptamine part but on the hexose part (Figure S10). To further confirm the production of DOP, we treated the reaction mixture with $NaBH_4$. HR-LC−MS analysis of the resulting mixture showed the disappearance of the signal corresponding to DOP (Figure 4A, trace (iii)) and formation of a new product with a protonated molecular ion at m/z = 308.1818 (1.3 ppm error for a calculated molecule formula of $C_{12}H_{25}N_3O_6$), corresponding to the reduced DOP (Figure 4A, trace (vi)). DOP (**4**) was apparently absent in the control assays in which SAM was omitted (Figure 4A, trace (i)). These results demonstrated that AprD4 is a radical SAM dehydratase, presenting a new example of radical-mediated chemically demanding dehydration reactions involving inactivated C−H bonds. Remarkably, except for the 3 AprD4 mutants with an impaired CX_3CX_3C motif, all the 9 Cys-to-Ala mutants converted paromamine to DOP, raising an intriguing question regarding the role of the auxiliary [4Fe-4S] cluster in the catalytic process.

We also probed the site for dAdo radical-mediated hydrogen abstraction by running the reaction in a buffer containing 67% D_2O. The result showed that deuterium incorporation into dAdoH was not apparent (Figure S11A), suggesting that the dAdo radical does not abstract a solvent-exchangeable hydrogen in AprD4 catalysis. However, we observed significant deuterium incorporation into the substrate (Figure S11B), indicating efficient reduction of the substrate radical by a solvent-derived hydrogen equivalent (Figure S11C). Similar observations were also found in the study of DesII[29,30] and NosL,[31] showing that deuterium was incorporated into the substrates when the reactions were performed in D_2O.

AprD3 Is an NADPH-Dependent Reductase. AprD3 shares high sequence similarities (BlastP E-values <1 × 10^{-40}) with many NADPH-dependent enzymes of the short chain dehydrogenase/reductase (SDR) family.[32] To investigate the function of AprD3, we knocked out its encoding gene by

DOI: 10.1021/jacs.6b02221
J. Am. Chem. Soc. 2016, 138, 6427−6435

targeted in-frame deletion (Figure S12). HPLC analysis showed that apramycin production was nearly abolished in the Δ*aprD3* mutant, and like the Δ*aprD4* mutant, this mutant also accumulated significant amounts of oxyapramycin and paromamine (~18 and 5 mg/L, respectively) (Figure 2, trace (iv)). Introduction of an *aprD3*-expressing plasmid into the Δ*aprD3* mutant dramatically diminished the production of oxyapramycin and paromamine, and restored apramycin production to the wide type level (Figure 2, trace (v)). These results clearly indicate that AprD3 is involved in C3 deoxygenation. Since the Δ*aprD3* mutant still produced a trace amount of apramycin (Figure 2, trace (iv)), the function of AprD3 may be partially complemented by some unknown enzymes from *S. tenebrarius*; similar enzyme functional complementation has been observed frequently in natural product biosynthesis (e.g., disruption of *encH*, *encI* or *encJ* did not abolished enterocin production[33]). Notably, we also observed a small amount of DOP (**4**) in the culture of the Δ*aprD3* mutant (Figure 4A, trace (iv)), and this is consistent with the AprD4 in vitro assays discussed above and suggested that DOP (**4**) is the likely substrate of AprD3.

We overexpressed AprD3 in *E. coli* with an N-terminal hexahistidine tag and performed a tandem reaction with both AprD4 and AprD3 in the presence of SAM, dithionite, paromamine, and NADPH. DOP was no longer observable in the reaction mixture (Figure 4A, trace (v)); instead, a large amount of a new compound with a protonated molecular ion at m/z = 308.1821 was produced (Figure 4A, trace (vii)). The suggested molecule formula of this product is $C_{12}H_{25}N_3O_6$ ($[M + H]^+$ calc. 308.1822, 0.3 ppm error), which is consistent with lividamine (**5**), a C3′ deoxygenated product of paromamine (Figure 4B). This compound was structurally validated by comparative HR-LC−MS/MS analysis (Figure S13) with the lividamine standard purified from the Δ*aprQ* mutant (vice infra) (Figure S14−16). These results clearly indicated that AprD3 is an NADPH-dependent reductase that works together with AprD4 to catalyze the C3′ deoxygenation of paromamine, establishing a new deoxygenation pathway in deoxy sugar biosynthesis. Notably, LC−MS analysis clearly showed that apramycin was not produced in an assay mixture containing oxyapramycin, AprD4, AprD3, and other required components, demonstrating that oxyapramycin is not an apramycin biosynthetic precursor as proposed previously (Figure 1), but is a final product produced by a pathway parallel to that for apramycin.

AprD3 and AprD4 Do Not Form a Tight Protein Complex. We noted that the yield of lividamine (**5**) produced in the tandem reaction with AprD4 and AprD3 is significantly higher (more than 10-fold roughly estimated according to the MS/MS intensities) than that of **4** produced in the AprD4-catalyzed reaction (Figure 4A), suggesting that AprD3 and AprD4 may function synergistically. In the C3 deoxygenation pathway in ascarylose biosynthesis (Figure S17), the dehydratase E1 and the reductase E3 form a catalytic complex and were coeluted in a FPLC gel-filtration analysis.[34] To investigate that whether AprD4 and AprD3 also form a catalytic complex, we incubated the two enzymes together and analyzed the resulting mixture by native-PAGE. No band corresponding to the comigration of AprD4 and AprD3 was observed in the analysis (Figure S18B), suggesting that these two enzymes do not form a tight protein complex. AprD4, AprD3, and the anaerobically incubated AprD4/AprD3 mixture were also analyzed by size exclusion fast protein liquid chromatography (FPLC), respectively, and the results are consistent with the native-PAGE analysis (Figure S18C). We further overexpressed AprD3 in *E. coli* with an N-terminal Flag tag and performed two sets of pull down assays, using anti-Flag tag and anti-His tag antibodies that target AprD3 and AprD4, respectively. No coimmunoprecipitation of AprD4 and AprD3 was observed in the two pull down assays (Figure 4C). These results exclude the possibility that the two enzymes form a tight protein complex. The low yield of DOP (**4**) in the reaction catalyzed by AprD4 alone is likely due to some feedback inhibition effect, and reduction of DOP (**4**) catalyzed by AprD3 may help to push the dehydration reaction forward. It also remains to be seen whether AprD4 and AprD3 form a transient complex and **4** is transferred directly from the AprD4 active site to AprD3, or alternatively, **4** is a diffusible reaction intermediate.

Lividamine Is the Substrate of the C6 Dehydrogenase AprQ. Most 2-DOS-containing AGAs have one or more hexoses that are aminated at the C6 position (Figure S19), and this C6 amination has been shown to be catalyzed by a FAD-dependent dehydrogenase and an aminotransferase.[35−38] In contrast, apramycin does not have a C6 amino group, and its biosynthetic gene cluster encodes a putative FAD-dependent dehydrogenase AprQ but lacks an aminotransferase gene. To interrogate the role of AprQ in apramycin biosynthesis, its encoding gene was knocked out by targeted in-frame deletion (Figure S2). LC−MS analysis showed that apramycin production was completely abolished in the Δ*aprQ* mutant, whereas a major product (~21 mg/L) exhibiting a protonated molecular ion at m/z = 308.1820 was produced (Figure 5, trace

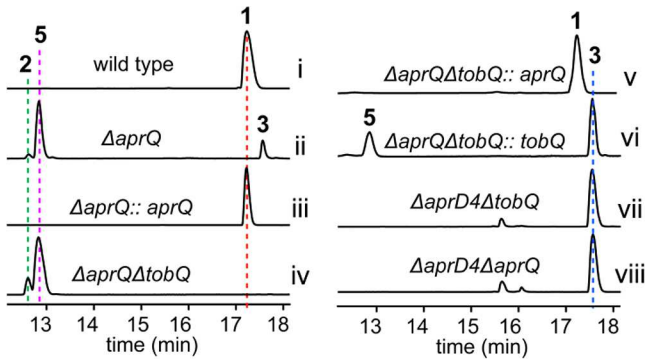

Figure 5. Functional dissection of AprQ and TobQ. (A) HPLC analysis of the culture extracts from (i) *S. tenebrarius* wild type strain, (ii) the Δ*aprQ* mutant strain, (iii) the Δ*aprQ* mutant containing an *aprQ*-expressing plasmid, (iv) the Δ*aprQ*Δ*tobQ* double-knockout mutant strain, (v) the Δ*aprQ*Δ*tobQ* double-knockout mutant strain containing an *aprQ*-expressing plasmid, (vi) the Δ*aprQ*Δ*tobQ* double-knockout mutant strain containing an *tobQ*-expressing plasmid, (vii) the Δ*aprD4*Δ*tobQ* double-knockout mutant strain, and (viii) the Δ*aprD4*Δ*aprQ* double-knockout mutant strain.

(ii)). This compound was structural validated to be lividamine (**5**) by HR-MS/MS, ^{1}H NMR, and ^{13}C NMR analysis of the purified compound (Figure S14−16). Introduction of an *aprQ*-overexpressing plasmid into the Δ*aprQ* mutant abolished lividamine production and restored apramycin production to the wild type level (Figure 5, trace (iii)), demonstrating the strict requirement of AprQ for apramycin biosynthesis.

Notably, the Δ*aprQ* mutant also produced oxyapramycin (**3**) and paromamine (**2**) (~4 and 1.5 mg/L, respectively) (Figure 5, trace (ii)). It has been previously shown that *S. tenebrarius* contains a gene cluster responsible for the biosynthesis of

DOI: 10.1021/jacs.6b02221
J. Am. Chem. Soc. 2016, 138, 6427−6435

tobramycin, an AGA that also contains a C3 deoxygenated hexose (Figure S19), but the *tob* gene cluster does not encode an AprD4 or AprD3 homologous protein.[39] It could be possible that TobQ encoded by the tobramycin biosynthetic gene cluster, which shares a high sequence similarity with AprQ (60% identity), was responsible for oxyapramycin production by the Δ*aprQ* mutant. To test this hypothesis, we constructed a Δ*aprQ*Δ*tobQ* double-knockout mutant strain by targeted in-frame deletions (Figure S21). Indeed, HPLC analysis showed that neither apramycin nor oxyapramycin was produced by the Δ*aprQ*Δ*tobQ* mutant (Figure 5, trace (iv)), and introduction of an *aprQ*-expressing plasmid into this mutant restored apramycin production to the wild type level (Figure 5, trace (v)). On the other hand, a mutant constructed by introduction of a *tobQ*-expressing plasmid into the Δ*aprQ*Δ*tobQ* mutant produced oxyapramycin and lividamine as the two major products, and apramycin was not observed in the culture of this mutant (Figure 5, trace (vi)). These results together suggested that lividamine is the substrate of AprQ but not the substrate of TobQ.

Both Lividamine and Paromamine Are the Substrates of AprQ. To study whether AprQ catalyzes the C6′ dehydrogenation of paromamine, we constructed the Δ*aprD4*Δ*tobQ* double-knockout mutant (Figure S22). HPLC analysis showed that this mutant produced a substantial amount of oxyapramycin (Figure 5, trace (vii)), suggesting that paromamine is also a substrate of AprQ. We also constructed the Δ*aprD4*Δ*aprQ* double-knockout mutant (Figure S23), and showed that both Δ*aprD4*Δ*tobQ* and Δ*aprD4*Δ*aprQ* mutants have a very similar metabolic profile (Figure, trace viii), suggesting that AprQ and TobQ likely have a similar catalytic efficiency on paromamine.

After several failed attempts in trying to express *aprQ* in *E. coli*, we finally chose *Streptomyces lividans* TK24 as a protein expression host, and by this way AprQ was successfully overexpressed with an N-terminal hexa-histidine tag and purified to homogeneity (Figure S24). Incubation of lividamine with AprQ resulted in a new product with a protonated molecular ion at m/z = 322.1602 (Figure 6A, trace (i)), and this product is absent in the control assays in which the supernatant of boiled enzyme was used (Figure 6A, trace (ii)). The suggested molecule formula $C_{12}H_{24}N_3O_7$ ($[M + H]^+$ calc. 322.1609, 2 ppm error) is consistent with 6′-hydroxyl-6′-oxolividamine (HOL, **6**), a lividamine analogue whose C6′ atom was oxidized to a carboxyl group (Figure 6B), and this compound was structurally validated by HR-MS/MS and NMR analysis (Figure S25–S26). Paromamine was also oxidized to 6′-hydroxyl-6′-oxoparomamine (HOP, **7**) (Figure 6B) in a similar way by AprQ (Figure 6A, trace (iii)–(iv), and Figure S27). These results are consistent with the gene knockout studies and confirmed that AprQ accepts both lividamine and paromamine as its substrates.

To investigate the substrate preference of AprQ, we performed a kinetic assay of AprQ for both lividamine and paromamine. The results showed that the catalytic efficiency (k_{cat}/K_m) of AprQ for lividamine was ~7.3-fold higher than that for paromamine, suggesting that lividamine is a preferred substrate of AprQ (Figure 6C). In contrary to ArpQ, we showed that TobQ converted paromamine to 6′-oxoparomamine (6-OP) but was not able to catalyze the oxidation of lividamine (Figure S28). These results are consistent with the knockout studies discussed above and suggested that paromamine is the substrate of TobQ whereas lividamine is not.

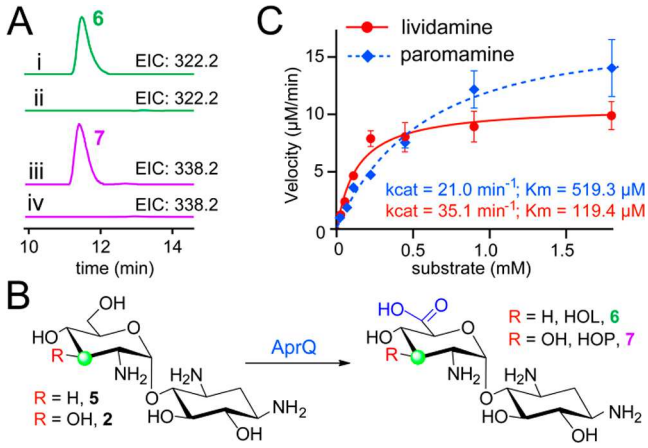

Figure 6. Both lividamine and paromamine are the substrates of AprQ. (A) LC–MS analysis of AprQ in vitro activity, showing the extracted ion chromatograms (EICs) of $[M + H]^+$ = 322.2 (corresponding to HOL, **6**) for (i) AprQ-catalyzed reaction with lividamine, and (ii) control reaction using lividamine and boiled AprQ; and the EICs of $[M + H]^+$ = 338.2 (corresponding to HOP, **7**) for (iii) AprQ-catalyzed reaction with paromamine, and (iv) control reaction using paromamine and boiled AprQ. (B) Both lividamine and paromamine were oxidized in the AprQ-catalyzed reactions. (C) The kinetic studies of AprQ with paromamine (blue trace) and lividamine (red trace) as substrates. The enzyme concentrations for assays with paromamine and lividamine are 1 μM and 0.3 μM, respectively. Assays were performed in triplicates and the standard deviations (S.D.) are shown by the error bars. HOL (**6**), 6′-hydroxyl-6′-oxolividamine; HOP (**7**), 6′-hydroxyl-6′-oxoparomamine.

Catalytic Versatility of AprQ. The distinct substrate specificity of AprQ and TobQ prompted us to perform a search for all the AprQ homologues in the NCBI database. This analysis identified 43 protein entries with BlastP E-values <1 × 10^{-80}, including 12 known C6 dehydrogenases involved in AGA biosynthesis and 31 uncharacterized AprQ homologues (Table S1). A Bayesian Markov chain Monte Carlo (MCMC) tree was constructed, and the tree shows that AprQ, TobQ, and KanQ are phylogenetically very close to each other and form a subclade in the tree (Figure 7A and Figure S29), consistent with the facts that these 3 enzymes all catalyze paromamine C6′ dehydrogenation. Notably, GenQ involved in the biosynthesis of gentamicins, which belong to the same 4,6-disubstituted 2-DOS-containing AGA subfamily as kanamycin (Figure S19), is phylogenetically far from TobQ and KanQ (Figure 7A). GenQ has been shown to catalyze the dehydrogenation of the pseudotrisaccharides gentamicin X2 and gentamicin G418,[38] and it remains unknown whether GenQ can also oxidize a pseudodisaccharide substrate. To answer this question, we expressed and purified GenQ and ran the in vitro assay separately with gentamicin X2, gentamicin G418, paromamine, and lividamine as the possible substrates. LC–MS analysis of the assay mixtures showed that both gentamicin X2 and gentamicin G418 were dehydrogenated by GenQ, whereas neither paromamine nor lividamine was dehydrogenated in the assay (Figure S30–S32). These results are consistent with the phylogenetic analysis and suggested that, unlike AprQ and TobQ, GenQ is not able to catalyze the dehydrogenation of pseudodisaccharide substrates. Intriguingly, when incubation gentamicin X2 or gentamicin G418 in the presence of AprQ, both substrates were dehydrogenated in the reaction (Figure 7B), demonstrating the remarkably broad substrate specificity

DOI: 10.1021/jacs.6b02221
J. Am. Chem. Soc. 2016, 138, 6427–6435

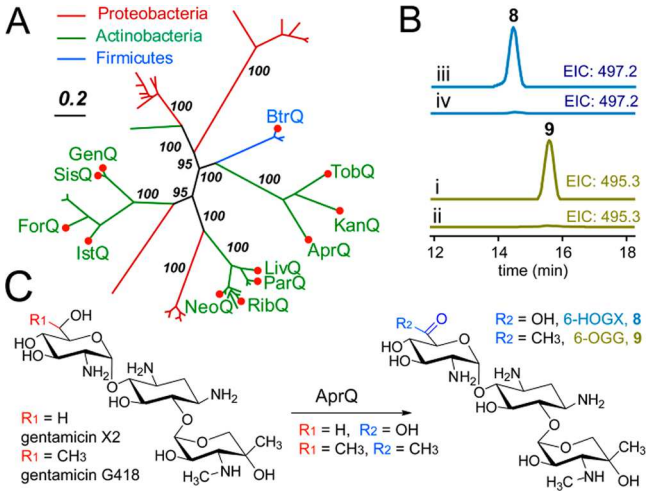

Figure 7. Catalytic versatility of AprQ. (A) A Bayesian MCMC tree of the AprQ homologous enzymes. Branches are colored according to their source organisms and only known enzymes are shown for clarity. The full tree is shown in Figure S29. (B) LC−MS analysis of AprQ in vitro assay with gentamicins, showing the EICs of $[M + H]^+$ = 497.2 (corresponding to 6-HOGX (**8**), the dehydrogenated product of gentamicin X2) for (i) AprQ-catalyzed reaction with gentamicin X2, and (ii) control reaction using gentamicin X2 and boiled AprQ; and the EICs of $[M + H]^+$ = 495.3 (corresponding to 6-OGG (**9**), the dehydrogenated product of gentamicin G418) for (iii) AprQ-catalyzed reaction with gentamicin G418, and (iv) control reaction using gentamicin G418 and boiled AprQ. (C) Scheme of the AprQ in vitro reactions with gentamicin G418 and gentamicin X2. 6-HOGX, 6′-hydroxyl-6′-oxogentamicin X2; 6-OGG, 6′-oxogentamicin G418.

of AprQ, which accepts not only different pseudodisaccharides but also pseudotrisaccharide substrates (Figure 7C).

DISCUSSION

Despite the decades-long clinical usage, AGAs still remain to be a valuable source for fighting against multidrug-resistant bacteria,[2,3] and their newly identified activities for the potential treatment of HIV[41] and human genetic diseases[42] are also attracting growing attentions in this old class of antibiotics. A detailed understanding of AGA biosynthesis serves as a prerequisite for guiding rational bioengineering efforts to produce novel AGAs. Although the apramycin biosynthetic gene cluster was reported more than a decade ago (Piepersberg et al., GenBank accession number AJ629123),[13] the biosynthetic pathway of apramycin remained largely elusive, and it has long been believed that C3 deoxygenation is the penultimate step in apramycin biosynthesis (Figure 1). However, our results demonstrate that paromamine is the substrate on which C3 deoxygenation occurs, and oxyapramycin is not a biosynthetic intermediate of apramycin but a final product resulted from a pathway parallel to that for apramycin (Figure 8).

Deoxygenation is normally essential for AGA activity by preventing enzyme modifications (e.g., phosphorylation, adenylation, and acetylation) on the hydroxyl group, which render the antibiotics inactive.[43,44] AGA-3′-phosphotransferase (APH (3′)) that phosphorylates the AGA C3 hydroxyl group, has been widely used as a selection marker in molecular biology. It has also been shown that oxyapramycin has 2- to 8-fold MICs than that of apramycin,[45] and C3′-deoxykanamycins have excellent activity against several kanamycin resistant bacteria,[46,47] demonstrating the importance of C3 deoxygenation for the AGA activity. The C3 deoxygenation pathway characterized in this study is apparently mechanistically different from that involved in ascarylose biosynthesis, which involves a pyridoxamine 5′-phosphate (PMP)-dependent and [2Fe-2S] containing enzyme (E1) and a [2Fe-2S] containing flavoprotein (E3) (Figure S17).[24,48]

The radical SAM-dependent chemistry of AprD4 is closely related to that of DesII, which was shown to be a poor dehydratase with an unnatural substrate.[29] AprD4 also appears to be related to the chemistry involved in ribonucleotide reductases, and the adenosylcobalamin-dependent diol dehydratases and ethanolamine amino lyase.[49−51] However, AprD4 is, to the best of our knowledge, the first radical SAM enzyme that has naturally evolved for a dehydratase activity. The sequential action of a radical SAM dehydratase and an NADPH-dependent reductase revealed in this study thus presents a novel paradigm in deoxy sugar biosynthesis.

This study also reveals a key branch point in AGA biosynthesis in *S. tenebrarius*, and demonstrates the functional

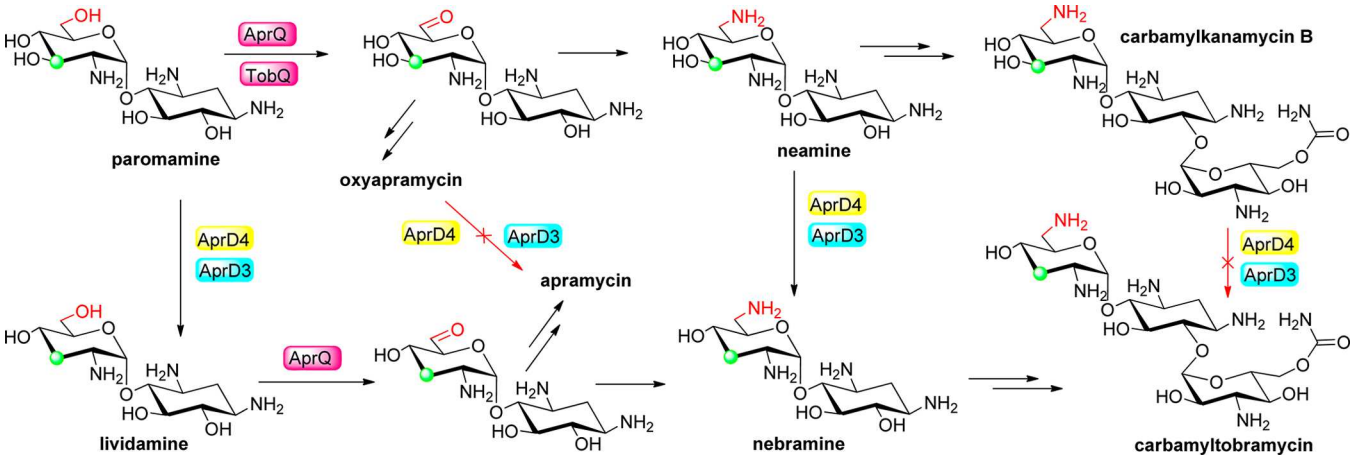

Figure 8. Paromamine serves as a key branch point intermediate in the combinatorial biosynthesis of AGAs in *S. tenebrarius*. Besides apramycin, and oxyapramycin, *S. tenebrarius* also produces carbamyltobramycin and carbamylkanamycin B, the carbamylated congeners of tobramycin and kanamycin B, respectively, as the minor constituents.[40] Conversion of neamine to nebramine was previously observed by using the cell free extract of *S. venezuelae* expressing *aprD4* and *aprD3*,[16] and this has been validated in our analysis using purified AprD4 and AprD3 (Figure S33).

DOI: 10.1021/jacs.6b02221
J. Am. Chem. Soc. 2016, 138, 6427−6435

complementarity and crosstalk between enzymes from different gene clusters (Figure 8). The newly identified parallel pathways in the biosynthesis of apramycin and tobramycin (Figure 8) complement the recent biosynthetic studies in kanamycin[16] and gentamicin[38,52] and suggest that parallel pathways are widespread in AGA biosynthesis, highlighting nature's ingenuity in accessing diverse natural products from a limited set of genes. The insights gleaned from the current investigation may thus facilitate further investigation of AGA biosynthesis and inspire future bioengineering efforts to generate novel sugar-containing natural products with improved activities.

While this work was under review, the Liu group also reported the successful reconstitution of the AprD4- and AprD3-catalyzed reactions.[53]

METHODS

Analysis of AGAs and Their Biosynthetic Intermediates. The culture supernatants of *S. tenebrarius* and its mutants were collected by centrifugation and adjusted to a pH of 2−3 with oxalate. After removal of the insoluble fraction by centrifugation at 5000 rpm for 30 min, the supernatant was passed through a column containing 5 mL 732 cation exchange resin (Hebi Juxing Resinco., Ltd.). The column was then washed with 50 mL of distilled water followed by 10 mL 3% ammonia hydroxide solution. The eluate was purged with a nitrogen stream and then taken to dryness by lyophilization. The residue was dissolved in 500 μL of H_2O before HPLC and LC−MS analysis. HPLC analysis were performed on a Dionex Ultimate 3000 system with evaporative light scattering detector (ELSD) (Alltech, 2000ES) equipped with a DIKMA Diamonsil C18 column (3.5 μm, 150 × 2.1 mm). The column was equilibrated with 80% solvent A (H_2O, 10 mM heptafluorobutyric acid) and 20% solvent B (CH_3CN), and developed with a gradient at a flow rate of 0.2 mL/min: 0−3 min, constant 80% A/20% B; 3−5 min, a linear gradient to 75% A/25% B; 5−9 min, a linear gradient to 71% A/29% B; 9−15 min, a linear gradient to 65% A/35% B, 15−20 min, a linear gradient to 62% A/38% B; 20−25 min, a linear gradient to 80% A/20% B.

Reconstitution of the [4Fe-4S] Cluster in AprD4. Chemical reconstitution of the [4Fe-4S] clusters of AprD4 and AprD4 mutants was performed under strictly anaerobic conditions, in a way similar to that previously used for NosL.[54] Briefly, freshly prepared dithiothreitol (DTT) was added to the purified protein fraction with a final concentration of 10 mM. $Fe(NH_4)_2(SO_4)_2$ solution (50 mM) was then added carefully to a final concentration of 1 mM. After 10 min of incubation at the room temperature, Na_2S solution (50 mM) was added in the same way to a final concentration of 1 mM. After further incubation on ice for 5−7 h, the resulting blackish solution was subjected to desalting on a DG-10 column (Bio-Rad) pre-equilibrated with the elution buffer I (50 mM MOPS, 25 mM NaCl, 10 mM DTT and 10% (v/v) glycerol, pH 8.0). The protein fraction was collected and concentrated, and was used directly for in vitro assay or stored at −80 °C upon further use.

Characterization of the [4Fe-4S] Cluster in AprD4. Quantification of Fe and S atoms per molecule of protein was performed in duplicate according to the methods described previously.[55,56] Protein concentration was determined using a Bradford assay kit (Promega) using bovine serum albumin as a standard. To record the UV−vis spectrum of AprD4, 200 μL of ∼25 μM reconstituted AprD4 was transferred into a quartz cuvette sealed with a rubber septa before taking the spectrum. The UV−vis spectrum of the reduced AprD4 was recorded similarly, using 200 μM of ∼25 μM AprD4 pretreated with 1 mM sodium dithionite at room temperature for 15 min. UV−vis spectroscopy analysis was performed on a 1900 double beam UV−vis spectrometer (Yoke Instrument Co. Ltd.).

AprD4 In Vitro Assay. AprD4 assays were carried out under strictly anaerobic conditions as described above. A typical assay was carried out by incubating 500 μM paromamine with ∼50 μM reconstituted AprD4 and 4 mM sodium dithionite in 50 mM MOPS buffer (pH 8.0) at room temperature for 10 min, and the reactions were initiated by addition of SAM to a final concentration of 1 mM. The assay mixtures were incubated at room temperature for ∼5 h, and the reactions were terminated by addition of trichloroacetic acid (TCA) to a final concentration of 10% (v/v). After removal of the protein precipitates by centrifugation, the supernatant was subjected to HPLC and/or LC−MS analysis. To perform the reaction in D_2O, 40 μL of precooled D_2O was carefully added to 20 μL of concentrated protein (∼100 μM) on ice, and the resulting protein solution (∼67% D_2O) was used directly for an assay with 100 μM paromamine, 1 mM sodium dithionite, and 500 μM SAM.

AprD4 and AprD3 Coupled Assay. The tandem reactions using both AprD3 and AprD4 were carried out similarly to AprD4 assay mentioned above. A typical assay mixture contains 500 μM substrate, ∼50 μM reconstituted AprD4, ∼20 μM AprD3, 4 mM sodium dithionite, and 1 mM NADPH in 50 mM MOPS buffer (pH 8.0).

Coimmunoprecipitation Experiments. For coimmunoprecipitation experiments AprD3 was overexpressed in *E. coli* with an N-terminal Flag tag. The AprD3-overexpression cell pellets from 20 mL culture were collected by centrifugation, washed twice with PBS (136 mM NaCl, 2.7 mM KCl, 10 mM Na_2HPO_4, 1.8 mM KH_2PO_4, pH 7.4), resuspended in 800 μL lysis buffer (50 mM MOPS, pH 8.0), and lysed by sonication (0.5 s on/4.5 s off cycle for 2 min). Cell debris was removed via centrifugation at 14 000 rpm for 10 min at 4 °C. Anti-His or anti-Flag pull down experiments were carried out by using anti-His Tag or anti-Flag Tag mouse monoclonal antibodies (Abbkine). Briefly, 100 μL AprD3 cell lysate, 50 μL reconstituted AprD4 (∼150 μM), and 2 μL anti-His Tag or anti-Flag Tag antibody were added together before anaerobic incubation at 4 °C for 2 h with gentle agitation. 35 μL of the protein G-coupled Sepharose beads (Fast Flow, Merck Millipore) were then added, and the resulting mixture was further incubated at 4 °C for 1.5 h with gentle agitation. The beads were then collected by centrifugation, washed four times by the lysis buffer, and boiled (100 °C) in 90 μL of 1× SDS-PAGE loading buffer (Vazyme) for 5 min. The supernatant was collected by centrifugation (5000 rpm, 3 min) and subjected to SDS-PAGE and Western blot analysis.

Expression of AprQ in *Streptomyces lividans* TK24. Construction of the AprQ-expressing *Streptomyces* strain WDY314 was detailed in Supporting Methods. For overexpression of AprQ, 200 μL spore suspension (10% glycerol) of WDY314 was used to inoculate 500 mL YEME medium containing 50 μg/mL apramycin, and the culture was grown at 28 °C (220 rpm) for 3 days. AprQ overexpression was initiated by addition of thiostrepton to a final concentration of 25 μg/mL, and the culture was grown for another 3 days. The cells were then harvested by centrifugation (5000 rpm, 30 min) and was used directly for protein purification or stored at −80 °C upon further use. To purify AprQ, the cells were resuspended in 40 mL lysis buffer (20 mM Tris, 300 mM NaCl, pH 8.0), and was lysed by a high pressure homogenizer (FB-110X, Shanghai Litu Mechanical Equipment Engineering Co., Ltd., China). Cell debris was removed by centrifugation at 14 000 rpm for 30 min at 4 °C. The supernatant was passed through a column of His-Binding Ni-NTA resin (GE Healthcare) pre-equilibrated with the lysis buffer, and was then subjected to affinity purification. The desired elution fractions were combined and concentrated using an Amicon Ultra-15 Centrifugal Filter Unit, and the concentrated protein solution was desalted using a DG-10 column (Bio-Rad) pre-equilibrated with the elution buffer II (20 mM Tris, 25 mM NaCl, and 10% (v/v) glycerol, pH 8.0). The protein fraction was collected and concentrated, analyzed by SDS-PAGE (10% Tris-glycine gel), and was used directly for in vitro assay or stored at −80 °C upon further use.

AprQ In Vitro Assay. A typical AprQ assay was carried out by incubating 100 μM substrate with ∼1 μM purified AprQ in 50 mM Tris buffer (pH 8.0) at 37 °C for 1 h, and the reactions were terminated by the addition of an equal volume of chloroform followed by vortexing. After removal of the protein precipitates by centrifugation, the aqueous phase was subjected to HPLC and/or LC−MS analysis. The kinetic study of AprQ was performed in 50 μL reaction mixtures with varied substrate concentration ranging from 25 μM to 1600 μM, and 0.3 μM and 1 μM AprQ were used separately for assays with lividamine and paromamine. After addition of the substrate

DOI: 10.1021/jacs.6b02221
J. Am. Chem. Soc. 2016, 138, 6427−6435

to a certain concentration, the reaction mixture was incubated at 37 °C for 10 min before addition of 50 μL of chloroform to terminate the reaction. The initial velocity was determined according to the decreased substrate concentration by selectively monitoring the intensity of the MS/MS fragmentation ion m/z = 163.1, with purified paromamine or lividamine serving as the external standards. Both substrate quantification and the reaction were performed in triplicates, and the results were analyzed by Thermo Xcalibur Quantitative Analysis. The resulting initial velocities were then fitted to the Michaelis–Menten equation by nonlinear regression analysis using Prism 6 (GraphPad software Inc.) to extract K_m and k_{cat} parameters. The analysis was performed in triplicates.

■ ASSOCIATED CONTENT

Supporting Information

The Supporting Information is available free of charge on the ACS Publications website at DOI: 10.1021/jacs.6b02221.

Experimental methods, additional figures and analyses. (PDF)

■ AUTHOR INFORMATION

Corresponding Authors

*yu_yi@whu.edu.cn

*qizhang@sioc.ac.cn

Author Contributions

#M.L. and X.J. contributed equally to this work.

Notes

The authors declare no competing financial interest.

■ ACKNOWLEDGMENTS

We thank Prof. Y. Sun (Wuhan University) for providing the *genQ* expression plasmid. Q.Z would also like to thank the Thousand Talents Program for support. This work was supported in part by grants from National Natural Science Foundation of China (31570033 to Y.Y., and 31500028 to Q.Z.), and from Fudan University (IDH1615002 to Q.Z).

■ REFERENCES

(1) Piepersberg, W.; Aboshanab, K.; Schmidt-Beissner, H.; Wehmeier, U. F. The biochemistry and genetics of aminoglycoside producers. In *Aminoglycoside Antiobiotics: From Chemical Biology to Drug Discovery*; Arya, D. P., Ed.; Wiley-Interscience: Hoboken, NJ, 2007; pp 15–118.

(2) Becker, B.; Cooper, M. A. *ACS Chem. Biol.* **2013**, *8*, 105.

(3) Jackson, J.; Chen, C.; Buising, K. *Curr. Opin. Infect. Dis.* **2013**, *26*, 516.

(4) Carter, A. P.; Clemons, W. M.; Brodersen, D. E.; Morgan-Warren, R. J.; Wimberly, B. T.; Ramakrishnan, V. *Nature* **2000**, *407*, 340.

(5) Han, Q.; Zhao, Q.; Fish, S.; Simonsen, K. B.; Vourloumis, D.; Froelich, J. M.; Wall, D.; Hermann, T. *Angew. Chem., Int. Ed.* **2005**, *44*, 2694.

(6) O'Connor, S.; Lam, L. K.; Jones, N. D.; Chaney, M. O. *J. Org. Chem.* **1976**, *41*, 2087.

(7) Denap, J. C.; Thomas, J. R.; Musk, D. J.; Hergenrother, P. J. *J. Am. Chem. Soc.* **2004**, *126*, 15402.

(8) Matt, T.; Ng, C. L.; Lang, K.; Sha, S. H.; Akbergenov, R.; Shcherbakov, D.; Meyer, M.; Duscha, S.; Xie, J.; Dubbaka, S. R.; Perez-Fernandez, D.; Vasella, A.; Ramakrishnan, V.; Schacht, J.; Bottger, E. C. *Proc. Natl. Acad. Sci. U. S. A.* **2012**, *109*, 10984.

(9) Mandhapati, A. R.; Shcherbakov, D.; Duscha, S.; Vasella, A.; Bottger, E. C.; Crich, D. *ChemMedChem* **2014**, *9*, 2074.

(10) Kudo, F.; Eguchi, T. *J. Antibiot.* **2009**, *62*, 471.

(11) Llewellyn, N. M.; Spencer, J. B. *Nat. Prod. Rep.* **2006**, *23*, 864.

(12) Park, S. R.; Park, J. W.; Ban, Y. H.; Sohng, J. K.; Yoon, Y. J. *Nat. Prod. Rep.* **2013**, *30*, 11.

(13) Wehmeier, U. F.; Piepersberg, W. *Methods Enzymol.* **2009**, *459*, 459.

(14) Lin, C. I.; McCarty, R. M.; Liu, H. W. *Chem. Soc. Rev.* **2013**, *42*, 4377.

(15) Ni, X.; Li, D.; Yang, L.; Huang, T.; Li, H.; Xia, H. *Appl. Microbiol. Biotechnol.* **2011**, *89*, 723.

(16) Park, J. W.; Park, S. R.; Nepal, K. K.; Han, A. R.; Ban, Y. H.; Yoo, Y. J.; Kim, E. J.; Kim, E. M.; Kim, D.; Sohng, J. K.; Yoon, Y. J. *Nat. Chem. Biol.* **2011**, *7*, 843.

(17) Schmerk, C. L.; Welander, P. V.; Hamad, M. A.; Bain, K. L.; Bernards, M. A.; Summons, R. E.; Valvano, M. A. *Environ. Microbiol.* **2015**, *17*, 735.

(18) Sofia, H. J.; Chen, G.; Hetzler, B. G.; Reyes-Spindola, J. F.; Miller, N. E. *Nucleic Acids Res.* **2001**, *29*, 1097.

(19) Frey, P. A.; Hegeman, A. D.; Ruzicka, F. J. *Crit. Rev. Biochem. Mol. Biol.* **2008**, *43*, 63.

(20) Booker, S. J.; Grove, T. L. *F1000 Biol. Rep* **2010**, *2*, 52.

(21) Broderick, J. B.; Duffus, B. R.; Duschene, K. S.; Shepard, E. M. *Chem. Rev.* **2014**, *114*, 4229.

(22) Bandarian, V. *Biochim. Biophys. Acta, Proteins Proteomics* **2012**, *1824*, 1245.

(23) Zhang, Q.; van der Donk, W. A.; Liu, W. *Acc. Chem. Res.* **2012**, *45*, 555.

(24) Ruszczycky, M. W.; Ogasawara, Y.; Liu, H. W. *Biochim. Biophys. Acta, Proteins Proteomics* **2012**, *1824*, 1231.

(25) Fluhe, L.; Marahiel, M. A. *Curr. Opin. Chem. Biol.* **2013**, *17*, 605.

(26) Wang, J.; Woldring, R. P.; Roman-Melendez, G. D.; McClain, A. M.; Alzua, B. R.; Marsh, E. N. *ACS Chem. Biol.* **2014**, *9*, 1929.

(27) Jarrett, J. T. *J. Biol. Chem.* **2015**, *290*, 3972.

(28) Mehta, A. P.; Abdelwahed, S. H.; Mahanta, N.; Fedoseyenko, D.; Philmus, B.; Cooper, L. E.; Liu, Y.; Jhulki, I.; Ealick, S. E.; Begley, T. P. *J. Biol. Chem.* **2015**, *290*, 3980.

(29) Ko, Y.; Ruszczycky, M. W.; Choi, S. H.; Liu, H. W. *Angew. Chem., Int. Ed.* **2015**, *54*, 860.

(30) Lin, G. M.; Choi, S. H.; Ruszczycky, M. W.; Liu, H. W. *J. Am. Chem. Soc.* **2015**, *137*, 4964.

(31) Ji, X. J.; Li, Y. Z.; Jia, Y. L.; Ding, W.; Zhang, Q. *Angew. Chem., Int. Ed.* **2016**, *55*, 3334.

(32) Oppermann, U.; Filling, C.; Hult, M.; Shafqat, N.; Wu, X.; Lindh, M.; Shafqat, J.; Nordling, E.; Kallberg, Y.; Persson, B.; Jornvall, H. *Chem.-Biol. Interact.* **2003**, *143–144*, 247.

(33) Xiang, L.; Moore, B. S. *J. Bacteriol.* **2003**, *185*, 399.

(34) Chen, X. M. H.; Ploux, O.; Liu, H. W. *Biochemistry* **1996**, *35*, 16412.

(35) Yu, Y.; Hou, X.; Ni, X.; Xia, H. *J. Antibiot.* **2008**, *61*, 63.

(36) Clausnitzer, D.; Piepersberg, W.; Wehmeier, U. F. *J. Appl. Microbiol.* **2011**, *111*, 642.

(37) Huang, F.; Spiteller, D.; Koorbanally, N. A.; Li, Y.; Llewellyn, N. M.; Spencer, J. B. *ChemBioChem* **2007**, *8*, 283.

(38) Guo, J.; Huang, F.; Huang, C.; Duan, X.; Jian, X.; Leeper, F.; Deng, Z.; Leadlay, P. F.; Sun, Y. *Chem. Biol.* **2014**, *21*, 608.

(39) Kharel, M. K.; Basnet, D. B.; Lee, H. C.; Liou, K.; Woo, J. S.; Kim, B. G.; Sohng, J. K. *FEMS Microbiol. Lett.* **2004**, *230*, 185.

(40) Koch, K. F.; Merkel, K. E.; Oconnor, S. C.; Occolowitz, J. L.; Paschal, J. W.; Dorman, D. E. *J. Org. Chem.* **1978**, *43*, 1430.

(41) Lapidot, A.; Berchanski, A.; Borkow, G. *FEBS J.* **2008**, *275*, 5236.

(42) Hainrichson, M.; Nudelman, I.; Baasov, T. *Org. Biomol. Chem.* **2008**, *6*, 227.

(43) Wright, G. D. *Curr. Opin. Microbiol.* **1999**, *2*, 499.

(44) Houghton, J. L.; Green, K. D.; Chen, W.; Garneau-Tsodikova, S. *ChemBioChem* **2010**, *11*, 880.

(45) Awata, M.; Satoi, S.; Muto, N.; Hayashi, M.; Sagai, H.; Sakakibara, H. *J. Antibiot.* **1983**, *36*, 651.

(46) Umezawa, S.; Tsuchiya, T.; Muto, R.; Nishimura, Y.; Umezawa, H. *J. Antibiot.* **1971**, *24*, 274.

(47) Kondo, S.; Hotta, K. *J. Infect. Chemother.* **1999**, *5*, 1.

DOI: 10.1021/jacs.6b02221
J. Am. Chem. Soc. 2016, 138, 6427–6435

(48) He, X.; Agnihotri, G.; Liu, H. H. W. *Chem. Rev.* **2000**, *100*, 4615.
(49) Bandarian, V.; Reed, G. H. In *The Chemistry and Biochemistry of B12*; Banerjee, R., Ed.; John Wiley: New York, 1999; p 811.
(50) Toraya, T. *Chem. Rev.* **2003**, *103*, 2095.
(51) Toraya, T. *Arch. Biochem. Biophys.* **2014**, *544*, 40.
(52) Huang, C.; Huang, F.; Moison, E.; Guo, J.; Jian, X.; Duan, X.; Deng, Z.; Leadlay, P. F.; Sun, Y. *Chem. Biol.* **2015**, *22*, 251.
(53) Kim, H. J.; LeVieux, J.; Yeh, Y. C.; Liu, H. W. *Angew. Chem., Int. Ed.* **2016**, *55*, 3724.
(54) Ji, X.; Li, Y.; Ding, W.; Zhang, Q. *Angew. Chem., Int. Ed.* **2015**, *54*, 9021.
(55) Kennedy, M. C.; Kent, T. A.; Emptage, M.; Merkle, H.; Beinert, H.; Munck, E. *J. Biol. Chem.* **1984**, *259*, 14463.
(56) Beinert, H. *Anal. Biochem.* **1983**, *131*, 373.

DOI: 10.1021/jacs.6b02221
J. Am. Chem. Soc. 2016, 138, 6427−6435